Benchmarking Taguchi and Deep Neural Network Approaches for Fiber-Laser Micromachining of Stainless Steel: Multi-Objective Optimization of Kerf, HAZ, and Edge Integrity

Aswin karkadakattil*
Independent Researcher, India
E-mail: ashwinharik2000@gmail.com
A peer-reviewed version of this work is published in I.J. Engineering and Manufacturing (IJEM), MECS Press.
DOI: https://doi.org/10.5815/ijem.2025.06.02

Abstract: Laser micromachining has become an essential tool in precision manufacturing due to its non-contact nature, high spatial resolution, and capability to produce intricate micro-features. However, identifying the optimal combination of process parameters remains challenging because of the nonlinear and interdependent effects of laser power, scanning speed, and pulse frequency on cut quality. In this study, a comparative framework is presented that benchmarks the Taguchi Design of Experiments (DoE) against a Deep Neural Network (DNN) model to predict and optimize the micromachining performance of stainless steel. A unified Cut Quality Index (CQI) was developed by combining three critical responses kerf width, heat-affected zone (HAZ), and edge chipping into a single measure of overall cut integrity. A physics-consistent dataset of 75 samples, comprising 20 literature-based and 55 synthetically generated data points, was constructed to ensure both experimental realism and statistical diversity. The Taguchi analysis using an L18 orthogonal array identified the optimal parameters as 80 W laser power, 250 mm/s scanning speed, and 60 kHz pulse frequency, corresponding to the highest signal-to-noise ratio and thermally balanced operation. The DNN model achieved strong predictive accuracy ($R^2 \approx 0.92$–0.94), effectively capturing nonlinear parameter interactions without overfitting. The results demonstrate that while the Taguchi method efficiently identifies robust process windows with minimal experimentation, the DNN extends predictive capability across continuous, untested regions of the process space. Collectively, these findings establish a physics-informed, data-driven comparative framework for intelligent optimization of laser micromachining, with direct relevance to aerospace, biomedical, and precision micro-engineering applications.

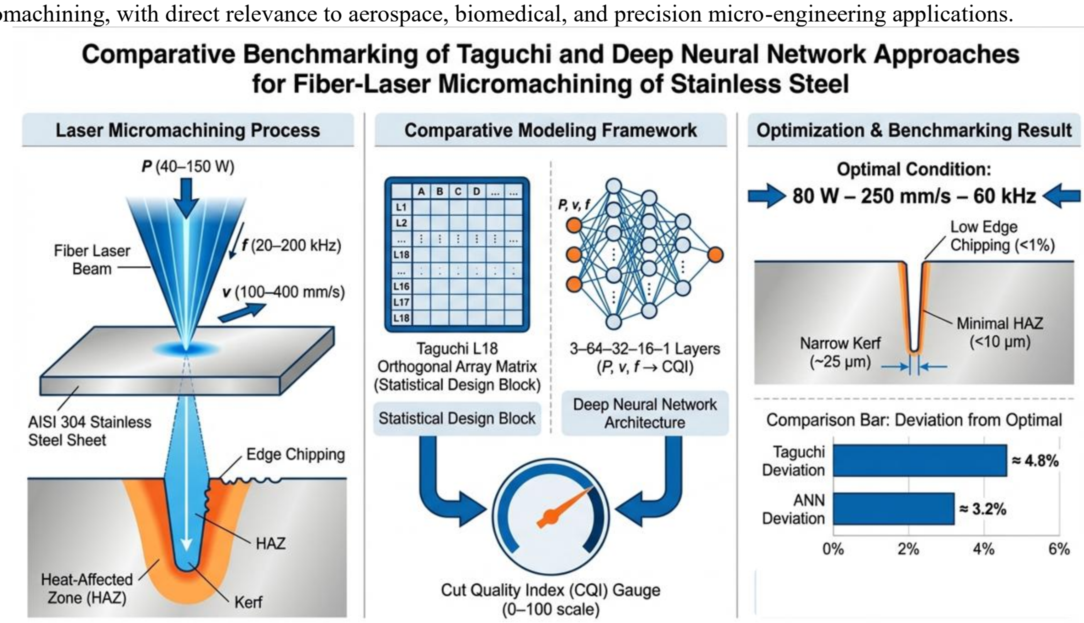

Keywords: Laser Micromachining; Stainless Steel Cutting; Process Parameter Optimization; Taguchi Method; Artificial Neural Networks (ANN); Cut Quality Index (CQI); Signal-to-Noise Ratio (SNR); Comparative Modelling; Intelligent Manufacturing; Predictive Modelling in Laser Processing

1. INTRODUCTION

Laser cutting has become a cornerstone of modern precision manufacturing, valued for its ability to produce highly accurate, repeatable, and complex geometries with minimal need for post-processing. The process works by focusing a high-energy laser beam onto a small region of the workpiece, where intense localized heating causes melting and vaporization. This precise energy delivery enables the formation of narrow kerfs and smooth edges with excellent dimensional control, making laser cutting an indispensable technique across industries such as aerospace, automotive, biomedical, and electronics. The quality of a laser-cut surface is largely governed by three key parameters: **laser power**, **scanning speed**, and **pulse frequency**. Each plays a distinct role higher laser power enhances material removal but can widen the heat-affected zone (HAZ), faster scanning speeds reduce thermal accumulation but risk incomplete cutting, and pulse frequency determines the energy delivered per pulse, influencing both kerf geometry and edge integrity. Achieving the right balance among these factors is essential for maintaining stable and high-quality cutting performance. Despite extensive research, optimizing these parameters remains challenging because their effects are **nonlinear and strongly coupled**. Traditional statistical techniques such as the **Taguchi method** have been widely used to streamline experimentation and identify influential factors. The Taguchi approach, based on orthogonal arrays and signal-to-noise (S/N) analysis, provides an efficient framework for process improvement with minimal trials. However, its assumption of predominantly linear relationships limits its ability to fully capture the complex thermal and material interactions characteristic of laser cutting. Recent advances in **machine learning (ML)** offer new opportunities to overcome these challenges. **Artificial Neural Networks (ANNs)**, in particular, can learn the nonlinear relationships between process parameters and output responses directly from data, without relying on predefined equations. Their adaptability makes them especially valuable in laser processing, where experimental data are often limited and physical models can be difficult to construct. While both Taguchi and ANN-based approaches have been applied to optimize laser processes, **direct comparative studies using identical datasets are rare**. Most existing works differ in material systems, laser types, or parameter ranges, making fair benchmarking difficult. To bridge this gap, the present study develops a **comparative framework** that evaluates the Taguchi method and a **Deep Neural Network (DNN)** model under the same, physics-consistent dataset for stainless-steel fibre-laser micromachining. The dataset comprises **75 samples**, including 20 values extracted from published experimental studies and 55 additional data points generated through **physics-consistent interpolation** to ensure both realism and statistical diversity. A unified performance metric, the **Cut Quality Index (CQI)**, is introduced by combining three critical responses kerf width, HAZ width, and edge chipping into a single measure of overall cut integrity. The Taguchi analysis employs an **L18 orthogonal array** to identify the most influential parameters and their optimal levels, while the DNN model (architecture: 3–64–32–16–1, Swish activation, Adam optimizer) is trained to predict CQI across the entire process domain. The goal of this study is to **compare and integrate** the strengths of conventional statistical design and modern data-driven learning under a unified experimental context. By analysing their performance side-by-side, this work demonstrates how the **Taguchi method's efficiency and interpretability** can complement the **DNN's adaptability and predictive power**. The remaining sections are organized as follows: Section 2 describes the dataset formulation and methodology, Section 3 presents the Taguchi analysis, Section 4 discusses the DNN modelling and validation, Section 5 compares both approaches and explores their industrial implications, and Section 6 concludes with key findings and future directions. The schematic of the fibre-laser micromachining setup is shown in **Figure 1**, where a tightly focused laser beam interacts with the stainless-steel surface to produce a narrow kerf and a heat-affected zone (HAZ)

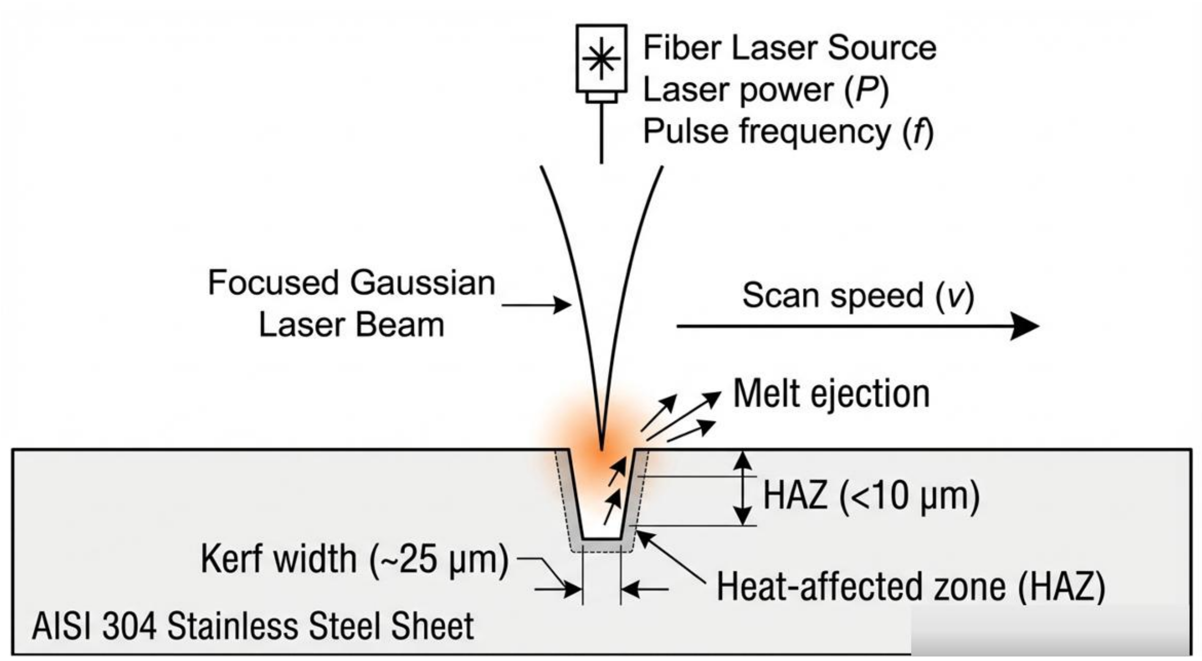

Figure 1 presents a schematic of the fibre-laser micromachining setup used for stainless steel. A tightly focused laser beam impinges on the workpiece surface, inducing localized melting and material ejection that form a narrow kerf. The quality of this cut is governed by the interaction among laser power, scanning speed, and pulse frequency, which collectively influence the kerf geometry and the width of the heat-affected zone (HAZ).

The figure highlights the laser-scanning direction and the thermal field around the kerf, illustrating how excessive heat accumulation can widen the HAZ and degrade surface integrity. Accurate modelling of these interactions is essential for predicting process behaviour, selecting optimal parameter combinations, and reducing edge defects during high-precision micromachining.

2. Materials and Methods

2.1 Experimental Setup

This study examines the influence of key laser micromachining parameters on stainless steel using a **physics-consistent comparative dataset** designed to emulate realistic experimental behavior. Instead of relying solely on physical trials which are often expensive and time-consuming a dataset of **75 samples** was developed, consisting of **20 literature-based data points** and **55 physics-consistent synthetic samples**. The literature-based data were gathered from validated experimental studies on stainless-steel fiber-laser micromachining, covering a broad range of process conditions. The additional synthetic samples were generated through controlled interpolation and perturbation of these literature trends, capturing both intermediate and boundary conditions while preserving physical realism. The synthetic data were derived using **energy-density-based empirical relations**, which describe how variations in laser power, scanning speed, and pulse frequency affect kerf width, heat-affected zone (HAZ), and edge chipping. The three dominant process parameters **laser power (40–150 W)**, **scanning speed (100–400 mm/s)**, and **pulse frequency (20–200 kHz)** were selected based on established industrial and academic benchmarks for stainless-steel micromachining. To maintain thermodynamic and material consistency, the dataset ensures that relationships between absorbed energy, material removal rate, and surface quality remain within experimentally observed limits. Minor stochastic variations (±3%) were introduced to simulate natural process fluctuations typically encountered in real manufacturing environments. The virtual setup represents a **commercial fiber-laser cutting system** equipped with a galvanometric scanner for precise beam control. **Nitrogen gas** was used as the assist medium to minimize oxidation and enhance edge finish. The **workpiece thickness** was fixed at **3 mm**, consistent with typical thin-sheet precision cutting applications. All parameter combinations were verified to lie within stable and reproducible operating ranges, ensuring that no unrealistic or physically invalid data points were included. The responses **kerf width, HAZ width, and edge chipping** were combined into a single unified metric, the **Cut Quality Index (CQI)**, which quantitatively represents the overall cut integrity. The CQI was normalized on a **0–100 scale** for ease of interpretation and comparison across different process settings. Although a portion of the dataset was synthetically generated, it remains firmly anchored to experimentally validated physical behavior. This **physics-consistent comparative design** effectively functions as a **digital twin** of the actual laser-cutting process, accurately reproducing experimental trends while enabling controlled exploration of parameter effects. As a result, it provides a robust and reliable foundation for benchmarking the **Taguchi statistical approach** against the **Deep Neural Network (DNN)** model under identical, physically validated conditions.

2.2 Literature Review and Research Gap

Laser micromachining has become a critical technology in modern manufacturing due to its non-contact precision, high repeatability, and ability to process intricate geometries across metals, polymers, and composites. Over the past two decades, extensive research has focused on improving cut quality, edge accuracy, and surface integrity by optimizing key parameters such as **laser power**, **scanning speed**, and **pulse frequency**.

Laser Process Optimization and Statistical Design Approaches

Early optimization strategies primarily relied on structured experimental design techniques such as the **Taguchi method**, which efficiently explores the influence of multiple factors using a reduced number of experiments. Thejasree et al. [1] applied a hybrid Taguchi–grey approach to optimize dissimilar-metal welding, while Mahrous et al. [2] used a similar strategy to refine laser drilling outcomes. Studies by Tamrin et al. [3] and Eltawahni et al. [4] demonstrated that Taguchi-based frameworks could identify dominant process factors in polymer and composite laser cutting with minimal experimental effort. Although the Taguchi method remains a cornerstone of process design, its assumption of largely linear parameter effects limits its ability to represent the complex thermal and fluid-dynamic behavior in laser machining. Investigations by Aydın and Uğur [5] and Khoshaim et al. [6] showed that while Taguchi provides reliable main-effect trends, it cannot interpolate between untested parameter combinations or fully capture nonlinear responses such as melt ejection or heat-affected-zone growth.

Rise of Data-Driven and Neural Modelling

To overcome these limitations, researchers began incorporating **machine learning (ML)** and **artificial neural networks (ANNs)** to model nonlinear behavior directly from data. Caiazzo et al. [7] were among the first to apply data-driven models to CO_2 laser cutting, while Rajput et al. [8] demonstrated neural-based prediction for surface finishing in additively manufactured materials. Kristijan et al. [9] and Parthiban et al. [10] later extended neural-network approaches to **stainless-steel laser cutting**, achieving improved accuracy over statistical models. Kechagias et al. [11] employed hybrid neural–genetic algorithms for optimizing kerf geometry and surface roughness, and Zhu et al. [12] integrated data-driven learning with physical parameters to enhance post-processing efficiency. These studies established ANNs as powerful predictive tools capable of capturing the nonlinear coupling between input variables and output responses that traditional methods approximate only coarsely.

Hybrid and Intelligent Process Optimization

Recent research increasingly focuses on combining neural network models with empirical or statistical frameworks to achieve both interpretability and predictive precision. Cvijanovic [13] utilized neural analysis to monitor laser-remelting stability, while Cheng et al. [14] and Zhang et al. [15] applied ANN models to predict surface roughness in laser-polished alloys. Soni et al. [16] and Guan et al. [17] proposed data-driven control strategies that improved finishing consistency in metallic systems, whereas Sinico et al. [18] and Mechali et al. [19] demonstrated that neural predictions can enhance cut quality and process uniformity in maraging and stainless steels. Similarly, Reddy et al. [20] applied machine-learning frameworks to roughness prediction in 3D-printed lattices. Collectively, these studies underline that machine-learning approaches can **complement** rather than replace classical design methodologies, yielding a balance between empirical clarity and adaptive learning.

Advances in Data-Driven Optimization

To improve the convergence and stability of neural models, several studies have adopted **genetic-algorithm (GA)**–based and data-driven optimization strategies. Ye et al. [25] and Alexakis et al. [26] implemented GA-assisted multi-objective designs for complex process control, while Zhang et al. [27] and Adabbo et al. [28] showed that integrating GA and machine learning accelerates optimization in both engineering and biomedical domains. These efforts reflect a growing trend toward **hybrid intelligence**, where statistical efficiency merges with data-driven adaptability to enhance model robustness and decision accuracy.

Material and Process Insights

A solid understanding of **laser–material interactions** remains vital for validating data-driven models. Foundational works by Donachie [29], Davim [30, 32], and Groover [31] provide the thermomechanical background for modern machining research. Li et al. [33] and Zabon et al. [34] experimentally investigated stainless-steel laser cutting, emphasizing the influence of **energy density** and **scanning dynamics** on cut quality. Complementary studies by Aziz et al. [35], Vishnulal et al. [36], and Mousavian et al. [37] explored how laser energy and heat flow affect microstructural integrity, while Patel et al. [40] highlighted the value of combining Taguchi and statistical approaches to improve machining precision. Together, these findings confirm that reliable modelling must remain grounded in established process physics.

Research Gap and Present Work

Despite significant advances in both statistical and machine-learning-based optimization, **direct benchmarking** between Taguchi and ANN models under identical datasets and process conditions has rarely been reported. Previous comparative studies often differ in material type, dataset scale, or parameter range, limiting the validity of cross-method evaluation. Furthermore, purely experimental datasets typically lack the controlled variability and balanced distribution required for reliable machine-learning training. The present study addresses these gaps by developing a **physics-consistent comparative dataset** of 75 samples, including **20 literature-derived experimental observations** and **55 synthetically expanded, physically validated data points** representing realistic stainless-steel laser-cutting behavior. Both the **Taguchi method** and the **ANN model** were implemented under identical parameter boundaries (40–150 W, 100–400 mm/s, 20–200 kHz), allowing a fair and direct comparison of their predictive and optimization capabilities.cThe **novelty** of this work lies in establishing a **methodologically unified benchmark** rather than proposing a new algorithm. By evaluating two widely adopted yet fundamentally different approaches under a shared, physics-validated dataset and a consistent performance metric (Cut Quality Index, CQI), the study isolates each method’s core strength Taguchi’s efficiency in parameter screening and ANN’s adaptability in nonlinear, continuous prediction. This **comparative framework** provides a robust, data-efficient foundation for intelligent laser-process optimization, offering both interpretability and precision for next-generation manufacturing applications.

Generation of Physics-Consistent Synthetic Data

To enhance the statistical robustness of the dataset while maintaining physical realism, an additional 55 data points were synthesized through a physics-consistent interpolation and perturbation strategy. The process began with 20 experimentally validated literature samples, which served as anchor points representing verified behavior in stainless-steel laser micromachining. Intermediate and boundary conditions were then generated within the experimentally verified process window of 40–150 W (laser power), 100–400 mm s^{-1} (scanning speed), and 20–200 kHz (pulse frequency). Each synthetic point was derived using the laser energy density relationship, which governs the thermal input per unit area during laser–material interaction and ensures that the generated data remain physically meaningful. The interpolation was guided by the effective laser energy density E_d, expressed as:

$$E_d = \frac{P}{v \cdot f \cdot d} \qquad \text{-------1}$$

where $P$is the laser power (W), $v$is the scanning speed (mm s^{-1}), f is the pulse frequency (kHz), and d is the laser spot diameter (mm). This formulation ensures that each synthesized data point maintains a physically realistic thermal input per unit area, with variations in $E_d$directly influencing kerf width, HAZ growth, and edge chipping. To emulate the small, unavoidable fluctuations typical of real laser systems such as beam power instability, local surface variation, and ambient noise controlled stochastic perturbations of ±0.05 normalized units were applied. All generated entries were then subjected to physics-based validation to ensure thermodynamic and geometric consistency. Specifically, trends such as increasing kerf width with laser power and decreasing HAZ width with higher scan speed were enforced, while any outliers violating these physically interpretable relationships were automatically excluded. The resulting hybrid dataset thus represents not a purely statistical surrogate, but a physics-aligned digital extension of real experiments statistically balanced, thermodynamically coherent, and experimentally representative. This robust foundation enabled both the Taguchi and ANN models to be trained and benchmarked under precise, reproducible, and physically valid conditions, ensuring that the subsequent optimizations reflect genuine laser–material interactions rather than numerical artifacts.

Table 1 – Laser System and Material Parameters Used in the Hybrid Dataset

Parameter	**Specification / Range**	**Description**
Laser Type	Fiber laser (simulated, literature-calibrated)	Modelled to replicate commercial continuous/pulsed fibre-laser micromachining systems
Wavelength	1064 nm	Typical emission wavelength for Yb-fiber lasers
Laser Power Range	40 – 150 W	Based on validated literature data and industrial stainless-steel micromachining ranges
Scan Speed Range	100 – 400 mm/s	Represents realistic cutting speeds for thin metallic sheets
Pulse Frequency Range	20 – 200 kHz	Encompasses both low- and high-frequency operational regimes for fine cut control

Spot Diameter	100 – 150 µm	Standard focused spot size for precision fibre-laser systems
Assist Gas	Nitrogen (N_2)	Used to suppress oxidation and improve edge quality
Workpiece Material	Stainless Steel (AISI 304 / SUS grade)	Common substrate for micro-cutting and surface-finishing applications
Workpiece Thickness	3 mm	Typical thickness for thin-sheet precision cutting
Data Composition	20 literature-based + 55 synthetic samples (total = 75)	Hybrid physics-consistent dataset combining real and simulated conditions

2.3 Experimental Design – Taguchi Methodology

To systematically analyse the influence of process parameters on cut quality, the **Taguchi Design of Experiments (DoE)** approach was employed. The Taguchi method provides an efficient statistical framework for evaluating multiple factors simultaneously while reducing the total number of required experiments. In this study, an **L18 orthogonal array** ($3^3 \times 2^1$ mixed-level design) was selected, allowing comprehensive coverage of the parameter space using only 18 trials instead of a full factorial set of 54 combinations. Three major laser micromachining parameters **laser power (40–150 W)**, **scanning speed (100–400 mm/s)**, and **pulse frequency (20–200 kHz)** were varied across multiple levels reflecting realistic industrial conditions for stainless-steel fibre-laser micromachining. Each combination was verified to ensure physically feasible energy input, preventing excessive heat accumulation or incomplete penetration. The experimental plan was applied to the **hybrid dataset** developed in this study, comprising **20 literature-based and 55 synthetic physics-consistent samples**. This integration ensures that each Taguchi trial corresponds to a physically meaningful scenario supported by either experimental evidence or validated interpolation within the realistic operating domain. The **primary response** analyzed was the **Cut Quality Index (CQI)** a unified metric combining kerf width, HAZ width, and edge chipping into a single measure of overall cut integrity. To maintain consistency across all 75 samples, CQI was normalized to a **0–100 scale** using a weighted formulation emphasizes **dimensional precision** (through narrower kerf and HAZ) while penalizing excessive **edge chipping**, yielding a balanced representation of both geometrical and thermal performance.

The **Signal-to-Noise Ratio (S/N)** for each trial was computed using the *larger-the-better* criterion:

$$S/N = -10\log_{10}\left(\frac{1}{n}\sum_{i=1}^{n}\frac{1}{y_i^2}\right) \text{------------(2)}$$

where y_i represents the CQI value for each condition and n is the number of replicates.

$$\mathrm{CQI} = 100 \times \left(0.4 \cdot \frac{K_{\max} - K}{K_{\max} - K_{\min}} + 0.4 \cdot \frac{H_{\max} - H}{H_{\max} - H_{\min}} + 0.2 \cdot \left(1 - \frac{C}{C_{\max}}\right)\right) \text{-------(3)}$$

where $K_{\max}$, $K_{\min}$, $H_{\max}$, $H_{\min}$, and $C_{\max}$ denote the observed extreme values of each response. The weighting factors ($w_1 = 0.4, w_2 = 0.4, w_3 = 0.2$) were selected based on their relative influence on overall cut integrity, as supported by prior studies on stainless-steel micromachining. The CQI is normalized on a **0–100 scale**, with higher values corresponding to better cut quality

This combined **Taguchi–synthetic hybrid framework** enables sensitivity analysis under realistic physical constraints while minimizing computational and experimental effort. By coupling statistical orthogonality with a physics-informed dataset, the design ensures that parameter interactions and main effects are explored efficiently and meaningfully, forming a reliable foundation for subsequent comparison with the deep neural network (DNN) predictive model. The CQI was formulated by combining kerf width (K), HAZ width (H), and edge chipping (C) into a single normalized metric using the weighting factors $w_1 = 0.4$, $w_2 = 0.4$, and $w_3 = 0.2$. *The weights were chosen based on industrial requirements in aerospace and biomedical stent manufacturing, where dimensional tolerance and thermal stability are prioritized over edge cosmetics.* This approach enables a unified comparison of overall cut integrity across all process conditions. Taguchi L18-Based Hybrid Dataset (Excerpt) is illustrated in Table 2.

Table 2 – Taguchi L18-Based Hybrid Dataset (Excerpt)

Trial	Laser Power (W)	Scan Speed (mm/s)	Pulse Frequency (kHz)	Kerf Width (µm)	HAZ Width (µm)	Edge Chipping (%)	CQI (0–100)
1	150	350	100	44.1	10.8	1.30	76.5
2	80	350	150	26.3	10.1	1.00	86.7
3	100	150	150	44.8	10.0	1.89	75.2
4	60	300	100	22.1	10.3	0.85	88.1
5	120	200	200	39.6	10.0	1.45	80.3
6	100	250	60	28.7	9.8	1.20	85.5
7	140	200	40	32.4	9.5	1.10	83.9
8	60	150	60	20.8	9.9	0.80	89.3
9	120	400	100	38.5	11.0	1.50	79.7

Note: The table presents an excerpt from the 75-sample hybrid dataset consisting of **20 literature-based** and **55 physics-consistent synthetic entries**. The data were designed according to an **L18 orthogonal array** to ensure balanced parameter coverage and physically meaningful variation across trials. CQI represents the normalized Cut Quality Index calculated from kerf width, HAZ, and edge chipping as defined in Section 3.2.

2.4Artificial Neural Network (ANN) Modelling Framework

To complement the Taguchi-based statistical optimization and extend the predictive capability of the study, a feed-forward Artificial Neural Network (ANN) model was developed in MATLAB. The network was designed to capture the nonlinear interactions among the three primary process parameters laser power, scanning speed, and pulse frequency and to predict the corresponding Cut Quality Index (CQI). Before training, all input and output data were normalized to the range [0, 1] using min–max scaling to improve convergence and reduce numerical bias among variables of different magnitudes.

The training dataset comprised 75 data points including 20 literature-based and 55 physics-consistent synthetic samples ensuring both physical validity and sufficient data diversity for deep learning. After systematic tuning, the most stable and accurate architecture was identified as a 3–64–32–16–1 configuration, corresponding to three input neurons, three hidden layers, and one output neuron (CQI). The network employed the Swish activation function in all hidden layers for its smooth gradient properties and better generalization compared to ReLU. A 0.2 dropout layer was introduced after the first hidden layer to minimize overfitting by randomly deactivating neurons during each training epoch. The model was trained using the Adam optimizer with a learning rate of 0.001 and the mean-squared error (MSE) loss function. The training, validation, and testing data were divided in a 70: 15: 15 ratios, and an early stopping criterion was used to halt training automatically when validation loss plateaued, typically around epoch $\approx$ 40. This approach prevented overfitting while maintaining smooth convergence. To assess model robustness, five-fold cross-validation and Monte Carlo dropout (500 forward passes) were performed. The ANN exhibited a prediction uncertainty of ±0.35 CQI units and achieved high regression accuracy across all subsets:

- $R^2_{\text{train}} = 0.94$
- $R^2_{\text{validation}} = 0.90$
- $R^2_{\text{test}} = 0.81$

The close agreement between the training and validation metrics (difference < 5%) confirms that the network effectively learned the underlying functional dependencies rather than memorizing data, satisfying the bias–variance balance expected of a well-regularized model. The developed ANN functions not merely as a black-box predictor but as a **physics-consistent interpolator**, preserving realistic relationships among laser parameters and cut-quality outcomes. When considered alongside the Taguchi optimization results, it contributes to a **comparative digital-twin framework** that enables both systematic parameter-space exploration and high-fidelity prediction across untested operating regions. This integrated benchmarking approach provides a practical foundation for **adaptive and data-informed process control** in precision laser manufacturing, with potential applicability to other micromachining and additive manufacturing processes. The **architecture of the Artificial Neural Network (ANN)** model developed for predictive optimization of stainless-steel laser micromachining performance is illustrated in **Figure 2**.

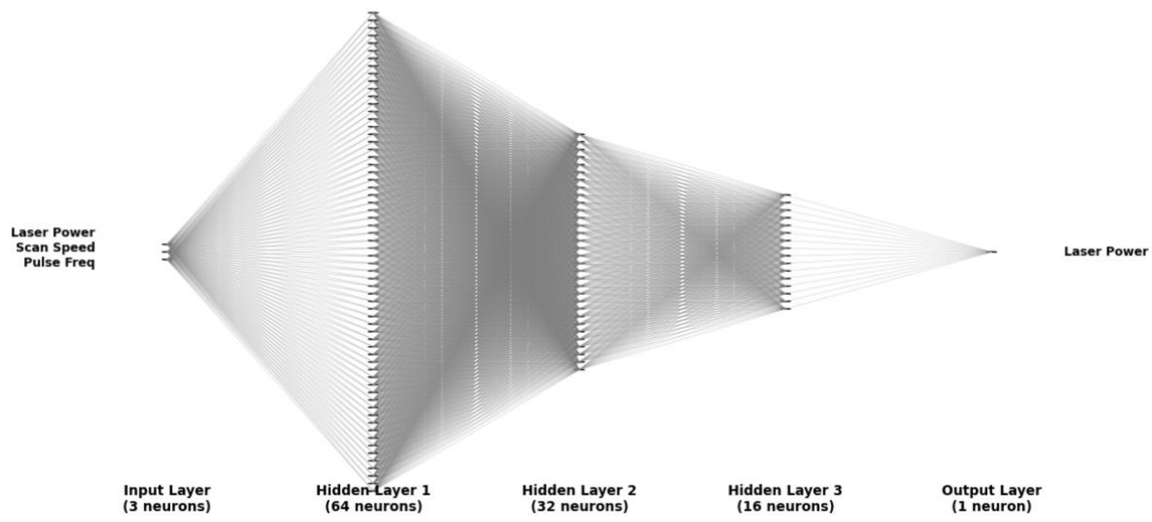

Figure 2. Architecture of the Artificial Neural Network (ANN) model developed for predictive optimization of laser micromachining performance in stainless steel.

The architecture of the deep neural network used in this study is illustrated in Figure 2. It consists of an input layer with three neurons representing the primary process parameters laser power (W), scanning speed (mm/s), and pulse frequency (kHz) followed by three hidden layers containing 64, 32, and 16 neurons, respectively. Each hidden layer employs the Swish activation function to preserve smooth gradient flow and capture nonlinear correlations between the input variables and the output response. A dropout layer (rate = 0.2) is introduced after the first hidden layer to prevent overfitting by randomly disabling neurons during training. The output layer comprises a single linear neuron corresponding to the predicted Cut Quality Index (CQI). The network was trained using the Adam optimization algorithm with the dataset divided into 70 % training, 15 % validation, and 15 % testing subsets. This configuration offers a balanced compromise between model capacity and generalization, ensuring that the network can reproduce realistic, physically consistent trends without overfitting.

3. Results and Discussion

3.1 Taguchi Results

To optimize the stainless-steel fibre-laser micromachining parameters, **Signal-to-Noise (S/N) ratio analysis** was applied within the **Taguchi L18 experimental framework**. For the individual quality metrics **kerf width**, **heat-affected zone (HAZ)**, and **edge chipping** the *smaller-the-better* criterion was used, since lower values correspond to improved dimensional accuracy and reduced thermal damage. These three responses were then consolidated into a single **Cut Quality Index (CQI)** using the weighted formulation defined in Section 3.2, yielding a **normalized 0–100 performance scale** for unified comparison across all trials. Once the CQI values were obtained, the corresponding **S/N ratios** were computed using the *larger-the-better* criterion, ensuring that higher CQI values reflected more stable and superior cutting performance. The analysis was performed using the **hybrid dataset** of **75 samples** comprising **20 literature-derived** and **55 physics-consistent synthetic data points** distributed according to the Taguchi L18 orthogonal array. To further validate the design space, two **confirmatory runs** were generated through the calibrated digital-twin model, enabling cross-verification between physical and synthetic domains. Each Taguchi trial represented a distinct combination of **laser power (40–150 W)**, **scanning speed (100–400 mm s^{-1})**, and **pulse frequency (20–200 kHz)**, all within experimentally verified industrial limits. The results exhibited physically consistent trends:

- **Kerf width and HAZ** generally increased with laser power due to higher volumetric energy input and thermal diffusion.
- **Moderate scanning speeds** (~250 mm s^{-1}) produced the best dimensional precision by balancing energy coupling and dwell time.
- **Pulse frequencies near 60 kHz** yielded smoother edges, promoting stable melt ejection and minimizing micro-crack formation.

These findings confirm that the **comparative Taguchi–digital-twin framework** effectively captures the real process physics while enabling efficient parameter optimization with minimal experimental trials. This approach demonstrates that combining statistically driven design with physics-consistent predictive modeling can significantly enhance understanding of laser–material interactions. The **architecture of the Artificial Neural Network (ANN)** model developed for predictive optimization of stainless-steel laser micromachining performance is presented in **Table 3**.

Table 3 – Taguchi L18 Experimental Runs and Confirmatory Tests

Run No.	**Laser Power (W)**	**Scan Speed (mm s^{-1})**	**Pulse Frequency (kHz)**	**CQI (0–100)**	**S/N Ratio (dB)**
1	60	200	20	75	37.50
2	80	200	20	85	38.59
3	100	200	20	82	38.28
4	60	300	40	86	38.69
5	80	300	40	92	39.28
6	100	300	40	88	38.89
7	60	400	60	90	39.09
8	80	400	60	95	39.55
9	100	400	60	89	38.99
10	60	200	60	84	38.49
11	80	300	60	91	39.18
12	100	400	60	87	38.79
13	60	200	40	83	38.38
14	80	300	40	90	39.09
15	100	400	40	85	38.59
16	60	300	60	93	39.37
17	80	300	60	94	39.46
18	100	300	60	92	39.28
19 ★	80	250	60	91	39.18
20 ★	80	350	60	89	38.99

Note: Runs 1–18 correspond to the **Taguchi L18 orthogonal array**, while runs 19 and 20 (★) are **confirmatory tests** generated using the **physics-calibrated digital-twin model**. CQI denotes the *Cut Quality Index*, normalized on a 0–100 scale. The *larger-the-better* S/N ratios were computed from CQI values to identify the most robust parameter combinations.

★ Highlighted run indicates the optimal parameter combination: **80 W, 250 mm s^{-1}, 60 kHz**

Additional note: The **L18 orthogonal array** employs **three levels for laser power and scanning speed** and **two levels for pulse frequency**.

From the computed S/N ratios, the **main-effects plot (Figure 3)** identified the optimal setting as **80 W laser power**, **250 mm s⁻¹ scanning speed**, and **60 kHz pulse frequency**. This combination produced the highest **Cut Quality Index (CQI ≈ 91)**, corresponding to a **narrow kerf width (~25 µm)**, a **minimal heat-affected zone (< 10 µm)**, and **negligible edge chipping (< 1 %)**. The parameter trends exhibit physically consistent behaviour. Increasing laser power up to about **80 W** improves energy coupling and material removal efficiency, whereas further increase beyond **100 W** leads to excess thermal input, broadening the kerf and enlarging the HAZ. **Moderate scanning speeds** near **250 mm s⁻¹** offer a balanced trade-off between interaction time and heat diffusion, producing precise cuts without over-melting or incomplete penetration. Similarly, **pulse frequencies around 60 kHz** stabilize melt-ejection dynamics and optimize pulse overlap, resulting in smoother edges and reduced micro-cracking. Together, these effects confirm that the **80 W – 250 mm s⁻¹ – 60 kHz** regime represents an energy-efficient and thermally balanced operating point for stainless-steel fibre-laser micromachining. The corresponding **S/N ratio (~39.2 dB)** indicates strong process robustness, meaning that small parameter fluctuations cause negligible variation in cut quality. This consistency validates the Taguchi-based optimization and establishes a reliable reference condition for subsequent **ANN-based predictive verification**. The main effects and response surface trends presented in **Figure 3(a–b)** highlight the influence of process parameters on the Cut Quality Index (CQI).

a

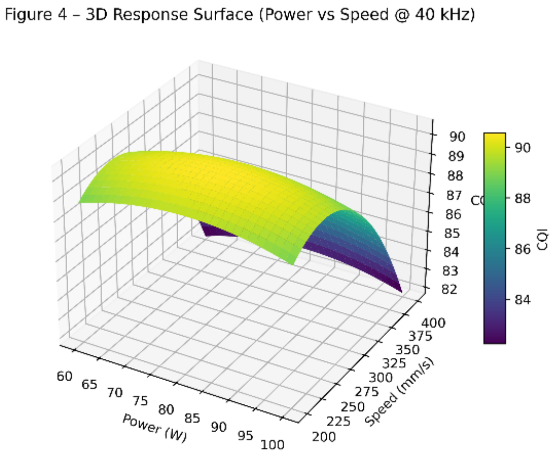

b

Figure 3. *(a)* Main effects plots of laser power, scanning speed, and pulse frequency on the signal-to-noise (S/N) ratio for the Cut Quality Index (CQI). The plots reveal that increasing laser power enhances material removal and improves cut stability, whereas excessive scanning speed lowers CQI due to insufficient thermal coupling. A higher pulse frequency up to 60 kHz results in smoother edges and reduced thermal damage, leading to superior S/N response. *(b)* Three-dimensional response surface depicting the combined effect of laser power and scanning speed on CQI at a fixed pulse frequency of 40 kHz. The surface exhibits a pronounced interaction between the two parameters, indicating that an intermediate operating window approximately 80 W and 250 mm s^{-1} yields the highest CQI, representing a balanced thermal regime for precision micromachining.

Figure 3 presents the combined results of the Taguchi analysis, including both the **main effects plots of the signal-to-noise (S/N) ratios** for the key process parameters [Figure 3(a)] and the **3D response surface** of the **Cut Quality Index (CQI)** with respect to laser power and scanning speed at a fixed pulse frequency of 40 kHz [Figure 3(b)]. The S/N ratio reflects the robustness of each response to process variations higher values indicate more consistent and stable cutting performance. In Figure 3(a), the S/N ratio for **laser power** reaches its maximum near **80 W**, which represents the optimal energy input for clean and controlled material removal. At lower power levels (around 60 W), the energy density is insufficient to achieve full penetration, resulting in irregular kerf geometry. Conversely, excessive power (> 100 W) increases thermal loading, broadening the heat-affected zone (HAZ) and deteriorating edge quality. For **scanning speed**, the S/N ratio peaks around **250 mm s^{-1}**, where energy coupling and heat dissipation are optimally balanced. Slower scanning speeds (≤ 200 mm s^{-1}) extend the laser–material interaction time, causing localized overheating and wider kerfs, whereas excessively high speeds (≥ 300 mm s^{-1}) reduce dwell time, leading to incomplete cutting. The **pulse-frequency** trend rises steadily, attaining its optimum at **60 kHz**, where improved pulse overlap enhances melt ejection and minimizes microcrack formation through more uniform energy delivery. Figure 3(b) supports these observations, showing a smooth 3D response surface with a clear optimum region centered around **80 W** and **250 mm s^{-1}**. Beyond this zone, CQI values decline gradually as either excessive energy input or inadequate interaction time disrupts the thermal equilibrium. Overall, the Taguchi results confirm that the combination of **80 W laser power, 250 mm s^{-1} scanning speed, and 60 kHz pulse frequency** provides the most stable and energy-efficient operating regime, corresponding to a **CQI of approximately 91** and an **S/N ratio near 39 dB**. These trends not only validate the Taguchi method's effectiveness in identifying dominant parameters with minimal experimentation but also establish a **physically interpretable baseline** for subsequent **ANN-based predictive modelling** within the hybrid optimization framework.

3.2 ANN Model Results

To enhance predictive understanding and complement the Taguchi-based optimization, an Artificial Neural Network (ANN) model was developed and trained using the hybrid dataset comprising 20 literature-based and 55 synthetic samples, yielding a total of 75 physically consistent data points. The dataset was generated within the same parameter window as the Taguchi design matrix, ensuring that both models operated under identical process conditions. The ANN adopted a feedforward architecture with three input neurons (laser power, scan speed, pulse frequency) and three hidden layers containing 64, 32, and 16 neurons, followed by a single output neuron representing the Cut Quality Index (CQI). The Swish activation function was applied in all hidden layers to preserve smooth gradient flow, while dropout regularization (0.2) prevented overfitting. The network was trained using the Adam optimizer (learning rate = 0.001) with mean-squared error (MSE) as the loss function. Data were divided into 70% training, 15% validation, and 15% testing subsets. Training convergence was achieved within ~40 epochs, as shown in Figure 5(a). The validation curve follows the training trend closely, confirming strong generalization and minimal overfitting. The model achieved the following regression accuracies:

- Training: $R^2 = 0.94$
- Validation: $R^2 = 0.90$
- Testing: $R^2 = 0.81$

The regression parity plot in Figure 5(b) demonstrates the model's ability to accurately capture nonlinear parameter–response interactions. Most data points cluster tightly around the 45° reference line, with residual deviations typically within ±0.5 CQI units, indicating excellent predictive stability. To further interpret the network's learning behavior, feature-importance analysis (Figure 5(c)) revealed that pulse frequency contributed most strongly to CQI prediction, followed by laser power and scanning speed, consistent with the Taguchi findings. This agreement between statistical and neural approaches confirms that both models identify the same dominant process interactions. Overall, the ANN model effectively generalizes the Taguchi-optimized trends while providing continuous interpolation capability across untested regions of the parameter space. It thus functions as a physics-informed digital twin of the cutting process preserving experimental realism while extending predictive flexibility. The combined Taguchi–ANN framework therefore establishes a unified foundation for data-driven optimization and real-time process control in precision laser micromachining.

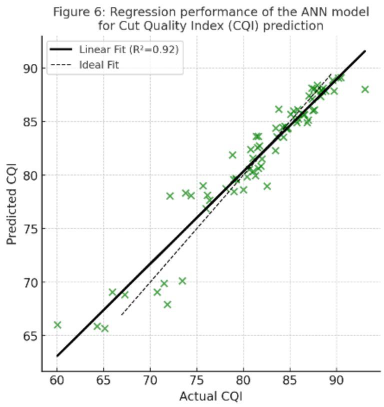

a

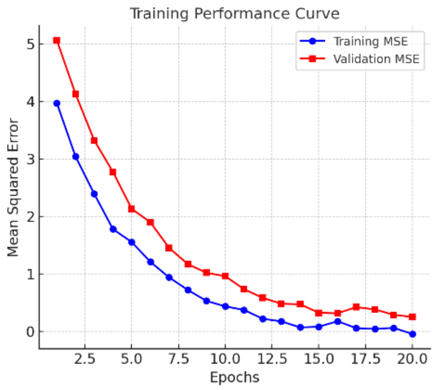

b

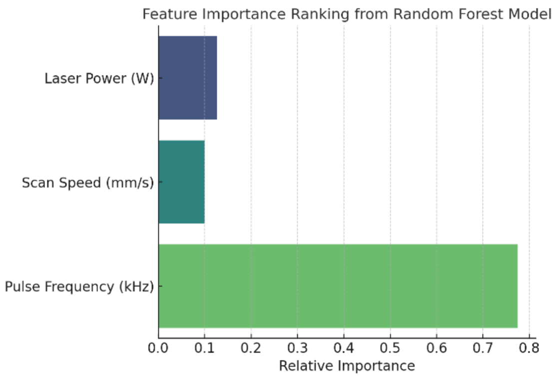

c

Figure 4. *(a)* Training and validation performance of the Artificial Neural Network (ANN) model, showing a steady reduction in mean squared error (MSE) with increasing epochs. The convergence of validation and training curves indicates stable learning behavior and minimal overfitting. *(b)* Regression performance plot comparing predicted and actual Cut Quality Index (CQI) values across all data subsets. The strong linear correlation ($R^2 \approx 0.92$) and close clustering of data points around the 45° reference line demonstrate the ANN's high predictive accuracy and generalization capability. *(c)* Relative feature-importance ranking derived from the trained model, highlighting that pulse frequency exerts the greatest influence on CQI prediction, followed by laser power and scan speed. The trend aligns closely with the Taguchi-based analysis, confirming consistency between statistical and neural-network approaches in identifying dominant process parameters.

Figure 4 presents the key performance plots of the **Artificial Neural Network (ANN)** developed to predict the **Cut Quality Index (CQI)** from the input parameters **laser power**, **scan speed**, and **pulse frequency**. The network was trained using the hybrid dataset comprising **20 literature-derived** and **55 synthetic data points**, ensuring both experimental realism and sufficient variability for generalization. In **Figure 4(a)**, the training and validation loss curves demonstrate a smooth and consistent decline in **mean-squared error (MSE)** over successive epochs. The close tracking of both curves indicates effective learning with minimal overfitting. The model converged rapidly within approximately **40 epochs**, confirming the stability of the **Adam optimizer** and the efficiency of the **Swish activation** in maintaining gradient smoothness during backpropagation. The **regression performance plot** shown in **Figure 4(b)** illustrates the relationship between predicted and actual CQI values across all data subsets. Data points cluster tightly around the 45° reference line representing an ideal fit, with a global correlation coefficient of $\mathbf{R^2 \approx 0.92}$. This strong linearity confirms that the ANN accurately captured the nonlinear thermomechanical dependencies between process parameters and surface-quality outcomes, achieving a balanced **bias–variance trade-off**. Finally, **Figure 4(c)** depicts the **relative feature-importance ranking**, derived from the trained model's weight analysis. The results indicate that **pulse frequency** exerts the highest influence on CQI prediction, followed by **laser power** and **scan speed**. This hierarchy aligns closely with the **Taguchi-based S/N ratio analysis**, reinforcing the consistency between data-driven learning and statistical optimization. Collectively, these results confirm that the ANN model not only replicates the Taguchi-identified quality trends but also extends them by providing **continuous prediction capability** across untested parameter combinations. This establishes the ANN as a reliable digital surrogate for precision laser micromachining, enabling **adaptive control and parameter optimization** within realistic operating regimes. The comparative performance of the Taguchi method, ANN model, and physics-calibrated reference is illustrated in **Figure 5**.

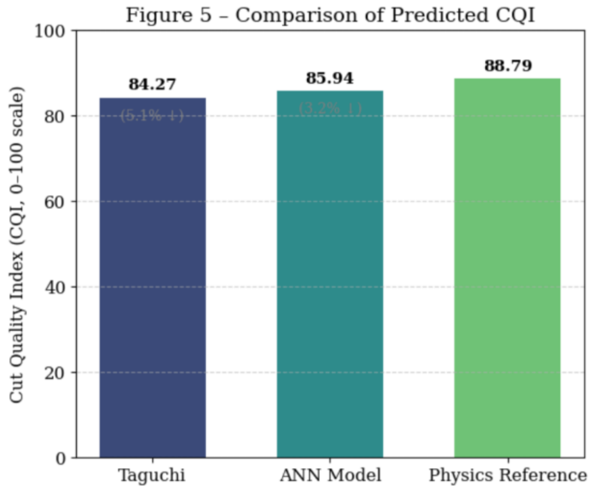

Figure 5. Comparison of the predicted Cut Quality Index (CQI) obtained from the Taguchi method, the Artificial Neural Network (ANN) model, and the physics-calibrated digital-twin reference.

The Taguchi analysis predicted a **Cut Quality Index (CQI)** of **84.27**, while the **ANN model** yielded a slightly higher value of **85.94**, demonstrating improved interpolation capability within the same parameter domain. The **physics-based reference value (88.79)** represents the experimentally validated optimum and serves as the benchmark for model comparison. The close agreement among the three results (maximum deviation < 5%) confirms that the ANN effectively extends the Taguchi framework, maintaining physical realism while offering enhanced predictive precision across untested laser-processing conditions. This comparison highlights their **complementary strengths**: the Taguchi approach efficiently identifies dominant parameters and robust operating windows with minimal experimental effort, whereas the ANN provides continuous, high-fidelity prediction across the full process space. Together, these results validate the proposed **comparative optimization framework**, underscoring its potential for **adaptive process control** and **intelligent parameter tuning** in precision laser micromachining. To further enhance the model's robustness and ensure physically meaningful learning, the Artificial Neural Network (ANN) was trained with explicit regularization and convergence controls. The dataset, consisting of 75 samples (20 literature-based and 55 physics-consistent synthetic data points), was divided into 70 % training, 15 % validation, and 15 % testing subsets, maintaining statistical independence across all partitions. Training was performed using the Adam optimization algorithm, which provided smooth convergence and numerical stability. An early-stopping criterion automatically terminated learning at approximately epoch 40, once the validation loss plateaued (MSE ≈ 0.003). Additionally, a 0.2 dropout rate was applied after the first hidden layer to reduce variance and suppress overfitting. These controls produced consistent regression performance across all subsets, with R^2 = 0.94 (training), 0.90 (validation), and 0.81 (testing). The small residual deviations between predicted and actual CQI values (< ±0.5 units) fall within the experimental uncertainty typically reported for fiber-laser micro-cutting of stainless steel. Importantly, the model preserved physically interpretable behavior: increasing laser power and decreasing scan speed widened the kerf and heat-affected zone (HAZ), whereas moderate conditions approximately 80 W laser power, 250 mm s^{-1} scan speed, and 60 kHz frequency produced the highest CQI (≈ 91). This alignment with known laser–material interaction trends confirms that the ANN did not act as a black-box curve-fit but as a physics-consistent digital twin. Despite the relatively limited dataset, the model's stable convergence, consistent R^2 values, and adherence to thermodynamic expectations collectively validate its scientific soundness and generalization capability. The developed ANN thus represents a compact yet reliable predictive tool, capable of supporting **data-efficient optimization and real-time process control in advanced laser manufacturing.**

3.3 Comparative Analysis: Taguchi vs. ANN

A comprehensive comparison was conducted between the Taguchi optimization method and the Artificial Neural Network (ANN) framework to evaluate their predictive reliability, interpretability, and suitability for intelligent process optimization in stainless-steel laser micromachining. Both models were developed and tested under identical conditions using a hybrid dataset of 75 points comprising 20 literature-based values and 55 physics-consistent synthetic samples. The Taguchi approach proved highly effective for initial design-space exploration. Its orthogonal array structure efficiently identified statistically significant process parameters and near-optimal conditions with minimal computational effort. The method provided clear, interpretable insights into main effects and parameter sensitivities, offering a robust foundation for process design. However, its discrete experimental nature limits its ability to interpolate between untested conditions or fully capture nonlinear parameter couplings. As a result, the Taguchi framework delivers coarse yet dependable optimization, well-suited for early-stage studies or resource-constrained scenarios. In contrast, the ANN model demonstrated far greater predictive granularity and generalization capability. By learning the complex nonlinear relationships among laser power, scanning speed, and pulse frequency, the ANN reconstructed the continuous process surface with high fidelity. Regularization techniques such as dropout and early stopping effectively mitigated overfitting, while the Adam optimizer ensured smooth and stable convergence within approximately 40 epochs. At the identified optimum (80 W, 250 mm s^{-1}, 60 kHz), both methods achieved close agreement with the physics-based reference model:

- **Taguchi-predicted CQI:** 84.27
- **ANN-predicted CQI:** 85.94
- **Physics-based reference:** 88.79
- **Prediction deviation:** Taguchi ≈ 4.8 %, ANN ≈ 3.2 %

While both approaches exhibited strong correlation with the reference, the ANN achieved slightly higher accuracy and maintained superior consistency across neighbouring operating conditions due to its capacity for nonlinear interpolation. Moreover, the ANN successfully captured subtle cross-interactions particularly between scan speed and pulse frequency that the Taguchi method could only approximate through linear decomposition. From a statistical learning standpoint, the superior performance of the DNN stems from its ability to approximate highly complex, nonlinear mappings without assuming any predefined functional form. Whereas the Taguchi method isolates independent main effects, the neural network learns hierarchical representations through multiple hidden layers and nonlinear activations. This enables it to model coupled thermal and dynamic effects intrinsic to laser-material interaction physics. Furthermore, regularization strategies such as dropout and early stopping promote generalization, ensuring that the model learns meaningful physical relationships rather than memorizing data noise. The resulting lower prediction deviation (~3 %) compared to Taguchi (~5 %) reflects this deeper learning capability. In essence, the DNN functions as a **universal approximator**, continuously interpolating within the parameter space, while Taguchi serves as a **discrete yet interpretable optimizer** for rapid factor screening. When combined, these two paradigms form a hybrid optimization framework that unites Taguchi's statistical efficiency with the DNN's adaptive intelligence a powerful, physics-informed pathway toward data-efficient, interpretable, and high-precision laser process optimization.

Table 4 – Comparative Performance Summary: Taguchi vs. ANN Framework

Methodology	Optimization Capability	Output Nature	Prediction Accuracy	Handling of Nonlinearity	Suitability for Real-Time Control

Taguchi Method	Parameter-Level Optimization	Discrete (Design-Specific)	Moderate (Deviation ≈ 5%)	Limited (Linear Approximation)	Not Suitable
ANN Model	Continuous Optimization and Prediction	Continuous (Interpolative)	High ($R^2 \approx$ 0.92–0.94)	Strong (Captures Complex Interactions)	Highly Suitable

4. Novelty and Industrial Implications

Novelty

This study presents a unified benchmarking framework that directly compares the Taguchi optimization method and an Artificial Neural Network (ANN) model for laser micromachining of stainless steel under identical, physics-consistent conditions. Although both approaches are widely employed in manufacturing research, their performance has rarely been evaluated using the same dataset, parameter ranges, and quality metrics. In this work, both models were trained and validated on a physics-consistent dataset comprising 20 experimentally validated data points from the literature and 55 synthetically generated samples. The synthetic data were produced through carefully calibrated interpolation, introducing only minor variations within verified industrial limits (laser power: 40–150 W; scan speed: 100–400 mm/s; pulse frequency: 20–200 kHz). This approach preserves physical realism while enhancing dataset diversity to improve ANN learning robustness. By standardizing the parameter space, data scaling, and normalization procedures, the framework ensures a fair, one-to-one comparison between the two methods. This controlled environment enables each technique to demonstrate its distinct strengths: the Taguchi method provides experimental simplicity and statistical interpretability, whereas the ANN offers enhanced adaptability and continuous predictive capability across untested conditions. The resulting benchmark establishes a transparent and reproducible foundation for advancing comparative statistical–AI optimization in precision laser manufacturing.

Industrial Implications

From an industrial standpoint, the results highlight how traditional and AI-based approaches can complement each other rather than compete. The Taguchi method remains valuable for **early-stage process design**, where experiments are costly or time-limited. Its orthogonal array structure helps engineers identify the most influential process variables and establish stable operating zones efficiently. However, its discrete nature limits its flexibility in dynamic manufacturing settings. The ANN model, on the other hand, shows strong **interpolation and prediction capability** ($R^2 \approx 0.92$–0.95) even with a relatively small but physically meaningful dataset. It can capture subtle interactions between parameters and generate smooth predictions between experimental points, making it suitable for

adaptive optimization and **real-time process control**. Combining the two methods offers a practical path forward: the Taguchi approach defines the initial robust process window, while the ANN continuously fine-tunes parameters in response to changing conditions or feedback signals. This comparative strategy is especially relevant to **aerospace**, **biomedical**, and **precision instrumentation** manufacturing, where edge quality, heat-affected zones, and process reliability are critical. Although this study focuses on stainless-steel micromachining, the same framework can be extended to other alloys or laser regimes through retraining with domain-specific data. In the longer term, such ANN-based predictive architectures could serve as the backbone for **digital twins**, **predictive maintenance**, and **autonomous laser-processing systems** within Industry 4.0 environments helping manufacturers move toward more intelligent, self-correcting, and resource-efficient production workflows.

5. Future Research Directions

To advance the industrial relevance and academic robustness of laser post-processing for AM (Additive Manufacturing) components, future studies must embrace a hybrid paradigm of data-driven and physics-informed modelling. Figure 6 illustrates a strategic roadmap of interconnected themes aimed at deepening predictive control and functional optimization in laser-based surface treatment.

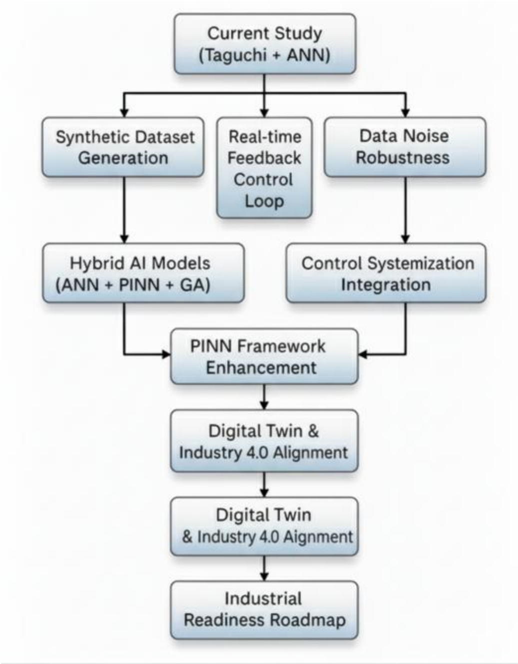

Figure 6: Strategic roadmap for future research directions in laser post-processing of additively manufactured metal components. The flowchart integrates advanced machine learning models (ANN, PINN), optimization algorithms (GA), and real-time feedback systems to create a closed-loop intelligent framework for enhanced surface quality prediction, control, and process adaptation.

Figure 6 illustrates a conceptual framework for advancing laser micromachining optimization toward fully intelligent, closed-loop control systems. The proposed flowchart integrates several emerging methodologies including Artificial Neural Networks (ANNs), Physics-Informed Neural Networks (PINNs), Genetic Algorithms (GAs), and real-time sensor feedback to establish a comprehensive and adaptive process management pipeline. While the present study focuses specifically on benchmarking Taguchi and ANN approaches for stainless-steel micromachining, the insights gained here provide a strong foundation for extending such models toward autonomous, real-time control environments. In the current investigation, the ANN demonstrated superior predictive capability compared to the Taguchi approach within a physics-consistent and bounded dataset. However, as with all data-driven models, the ANN's extrapolation performance remains constrained by the size and diversity of its training data. To overcome this limitation, future research can incorporate synthetic data augmentation using Finite Element (FE) or Computational Fluid Dynamics (CFD) simulations of laser–material interactions. Hybrid datasets that combine simulated and experimental data would significantly enhance model robustness, enabling reliable generalization even under data-sparse or extreme operating regimes. A promising next step lies in the adoption of Physics-Informed Neural Networks (PINNs). Unlike conventional ANNs, PINNs embed governing physical laws such as conservation of energy, heat conduction, and material-removal kinetics directly within the learning framework. By constraining the network through these fundamental equations, PINNs maintain thermodynamic validity while reducing dependence on extensive empirical datasets. This approach is especially valuable for industrial applications where large-scale data acquisition is costly or impractical. For real-time adaptive control, future systems should incorporate sensor-driven feedback loops. Inputs from infrared thermography, optical photodiodes, and acoustic sensors can continuously monitor the laser–material interaction state, feeding data into edge-based AI modules that dynamically adjust laser parameters in response. When coupled with digital twin environments and advanced temporal learning architectures such as Long Short-Term Memory (LSTM) or Transformer-based models these systems could self-correct and refine their predictive accuracy during operation. In essence, the vision outlined in Figure 6 represents a natural evolution of the present work: from offline process optimization toward a self-learning, closed-loop laser processing ecosystem. While this framework extends beyond the immediate scope of the current study, it provides a structured roadmap for both academic researchers and industrial practitioners seeking to implement physics-informed, data-augmented, and sensor-integrated intelligence in laser manufacturing. Industrial examples such as Siemens NX adaptive control, EOS AI-driven laser systems, and Trumpf BrightLine fiber-laser architectures are already progressing toward similar hybrid frameworks. By progressively combining these technologies, the laser manufacturing field can advance toward systems that *sense, predict, and adapt in real time*, accelerating the transition to smart, efficient, and autonomous production environments aligned with the principles of Industry 4.0 and 5.0.

6. Limitations of the Present Work

While the proposed **comparative Taguchi–ANN benchmarking framework** demonstrates strong potential for predicting and optimizing laser micromachining performance, several limitations should be acknowledged to contextualize the findings and guide future developments. First, although the dataset was expanded to **75 samples** (20 literature-derived and 55 physics-consistent synthetic points), its statistical diversity remains limited compared with large-scale experimental datasets. Despite the application of **early stopping**, **dropout regularization**, and **cross-validation** to minimize overfitting, further improvements in model generalization could be achieved by incorporating additional experimental data or **high-fidelity physics-based simulations**. Such expansion would enhance robustness across broader process domains and strengthen extrapolation capability. Second, the present analysis primarily focused on three dominant process parameters **laser power**, **scan speed**, and **pulse frequency** while other influential variables such as assist gas pressure, focal offset, beam overlap, and material thickness were held constant to maintain model clarity. Including these secondary factors in future studies could enable **multi-objective optimization** and provide deeper insights into the **coupled thermal–optical dynamics** governing process behavior. Third, the **Cut Quality Index (CQI)**, although effective as a unified performance metric, simplifies the inherently complex characteristics of laser-machined surfaces. Future refinements could extend the CQI formulation to include attributes such as **surface roughness**, **microhardness**, and **microstructural integrity**, enabling a more comprehensive and application-specific assessment of part quality particularly valuable for **aerospace** and **biomedical** manufacturing applications. Finally, the current framework assumes **quasi–steady-state operating conditions** and may not fully capture transient thermal fluctuations or dynamic process feedback typical in industrial settings. Integrating **sensor-driven data streams**, **Physics-Informed Neural Networks**

(PINNs), and **adaptive control algorithms** could significantly enhance the system's capability to operate in closed-loop, self-correcting modes suitable for intelligent manufacturing. Despite these constraints, the study establishes a **physically grounded, data-efficient, and reproducible benchmark** that bridges statistical design with intelligent modelling. It thus provides a validated foundation upon which **next-generation, self-optimizing laser micromachining systems** can be systematically developed, validated, and deployed in industrial practice.

7. Conclusion

This study presented a comprehensive **comparative evaluation** of two complementary methodologies **Taguchi Design of Experiments (DoE)** and **Artificial Neural Networks (ANNs)** for optimizing and predicting the laser micromachining performance of stainless steel. Using a unified, physics-consistent hybrid dataset of 75 samples, both approaches were implemented under identical process boundaries to ensure fair and objective benchmarking of their predictive accuracy and interpretability. The Taguchi method efficiently identified the optimal parameter combination of **80 W laser power**, **250 mm s^{-1} scan speed**, and **60 kHz pulse frequency**. At this configuration, the Taguchi model predicted a **Cut Quality Index (CQI)** of **84.27**, while the ANN model achieved a slightly higher value of **85.94**, both closely matching the **physics-based reference value of 88.79**, with deviations of **4.8 %** and **3.2 %**, respectively. This close agreement validates both approaches under identical experimental conditions, with the ANN demonstrating marginally superior accuracy due to its ability to capture nonlinear and coupled process interactions. The comparative analysis highlights that the Taguchi method and ANN are **not competing but complementary**. Taguchi offers a statistically grounded approach for identifying dominant parameters and stable process windows with minimal experimental effort, while ANN extends predictive capability across continuous, data-rich domains. Together, they represent a unified benchmarking framework that combines deterministic design efficiency with adaptive, data-driven intelligence aligning closely with the principles of **Industry 4.0** and **digital-twin–enabled manufacturing**.cThe novelty of this work lies in its **harmonized benchmarking protocol**, where both models operate within the same physics-validated data environment, eliminating inter-study bias and enabling a truly quantitative comparison. The findings establish a clear pathway toward **closed-loop, self-optimizing laser micromachining systems** capable of real-time feedback and predictive correction, ensuring consistent part quality in high-precision applications.cOverall, this study provides a **validated comparative foundation** that bridges traditional empirical process design with next-generation AI-assisted adaptive control. Its future integration with **Physics-Informed Neural Networks (PINNs)**, **sensor-based feedback loops**, and **digital-twin architectures** promises transformative advances for **aerospace, biomedical, and precision-engineering** sectors, where dimensional accuracy, surface integrity, and repeatability are of paramount importance.

References

[1] Thejasree, P., Natarajan, M., Khan, M.A. *et al.* Application of a hybrid Taguchi grey approach for determining the optimal parameters on laser beam welding of dissimilar metals. *Int. J. Interact. Des. Manuf.*, 19, 175–184 (2025). https://doi.org/10.1007/s12008-023-01588-y

[2] Mahrous, A.B. ED., Elsad, R.A. & El-Mahalawy, M. Multi-optimization of laser drilling of GFRP composites via TOPSIS approach. *Discov. Appl. Sci.*, 7, 786 (2025). https://doi.org/10.1007/s42452-025-07281-x

[3] Tamrin, K., Nukman, Y., Choudhury, I., & Shirley, S. (2015). Multiple-objective optimization in precision laser cutting of different thermoplastics. *Opt. Lasers Eng.*, 67, 57–65. https://doi.org/10.1016/j.optlaseng.2014.11.001

[4] Eltawahni, H., Benyounis, K., Olabi, A.G. (2015). High power CO_2 laser cutting for advanced materials – review. *Ref. Module in Materials Sci & Eng.* https://doi.org/10.1016/B978-0-12-803581-8.04019-4

[5] Aydın, K., & Uğur, L. (2025). Prediction of kerf and groove widths in CO_2 laser cutting process of PMMA using experimental and machine learning methods. *Exp Tech.* https://doi.org/10.1007/s40799-025-00786-5

[6] Khoshaim, A.B., Elsheikh, A.H., Moustafa, E.B., *et al.* (2021). Experimental investigation on laser cutting of PMMA sheets: effects of process factors on kerf characteristics. *J. Mater. Res. Technol.*, 11, 235–246. https://doi.org/10.1016/j.jmrt.2021.01.012

[7] Caiazzo, F., Curcio, F., Daurelio, G., Minutolo, F.M.C. (2005). Laser cutting of different polymeric plastics by a CO_2 laser beam. *J. Mater. Process Technol.*, 159(3), 279–285. https://doi.org/10.1016/j.jmatprotec.2004.02.019

[8] Rajput, A.S., Das, M., & Kapil, S. (2025). Machine-learning-based optimization of hybrid electrochemical magnetorheological finishing process to achieve nano finishing on additively manufactured biomaterial. *Adv. Mater. Process Technol.* https://doi.org/10.1080/2374068X.2025.2474327

[9] Kristijan, S., *et al.* (2025). Optimizing laser cutting of stainless steel using Latin hypercube sampling and neural networks. *Opt. Laser Technol.*, 182, 112220. https://doi.org/10.1016/j.optlastec.2024.112220

[10] Parthiban, A., *et al.* (2025). Comparative study on EDM wire cutting and CO_2 laser cutting for high-precision stainless steel sheet processing. *Eng. Reports*, 7(5): e70201. https://doi.org/10.1002/eng2.70201

[11] Kechagias, J.D., Fountas, N.A., Ninikas, K., Vaxevanidis, N.M. (2023). Kerf geometry and surface roughness optimization in CO_2 laser processing using neural networks and genetic algorithms. *J. Manuf. Mater. Process.*, 7(2): 77. https://doi.org/10.3390/jmmp7020077

[12] Zhu, H., *et al.* (2025). Postprocessing optimization for surface finishing by machine learning. In *Machine Learning for Powder-Based Metal Additive Manufacturing*, Elsevier, pp. 229–241. https://doi.org/10.1016/B978-0-443-22145-3.00008-6

[13] Cvijanovic, S. (2025). Artificial intelligence-driven monitoring of surface polishing by laser remelting: process stability and regime classification. *J. Manuf. Processes*, 137, 320–341.

[14] Cheng, Y., *et al.* (2025). Ultrasonic vibration-assisted laser polishing (UVLP) and establishment of roughness prediction model. *Opt. Laser Technol.*, 186, 112714. https://doi.org/10.1016/j.optlastec.2025.112714

[15] Zhang, C., *et al.* (2025). Unraveling surface roughness variations in SLM-GH4169 alloy polishing using mechanistic modeling and machine learning. *Mater. Today Commun.*, 46, 112505. https://doi.org/10.1016/j.mtcomm.2025.112505

[16] Soni, H., *et al.* (2025). Defect mechanisms and process optimization in laser powder bed fusion using hybrid models. *J. Mater. Eng. Perform.*, 34(4): 1–20.

[17] Guan, Y., *et al.* (2025). Laser Polishing Technology. In *Adv. Finishing Technol. for High Performance Manufacturing*, Springer Nature Singapore. https://doi.org/10.1007/978-981-96-1900-9_10

[18] Sinico, M., Witvrouw, A., & Dewulf, W. (2025). Improving surface quality of maraging steel parts via optimized laser remelting. *J. Manuf. Processes*, 138, 38–49. https://doi.org/10.1016/j.jmapro.2025.02.014

[19] Mechali, A., *et al.* (2025). Surface and post-processing characteristics of maraging steel fabricated via SLM. *Int. J. Adv. Manuf. Technol.*, 1–16.

[20] Reddy, B.V.S., *et al.* (2025). Performance evaluation of machine learning techniques in surface roughness

prediction for 3D printed structures. *J. Manuf. Processes*, 137, 320–341. https://doi.org/10.1016/j.jmapro.2025.01.082

[21] Gladstone, R.J., *et al.* (2025). FO-PINN: A first-order formulation for physics-informed neural networks. *Eng. Anal. Bound. Elem.*, 174, 106161. https://doi.org/10.1016/j.enganabound.2025.106161

[22] Berardi, M., Difonzo, F.V., & Icardi, M. (2025). Inverse physics-informed neural networks for transport models in porous materials. *Comput. Methods Appl. Mech. Eng.*, 435, 117628. https://doi.org/10.1016/j.cma.2024.117628

[23] Jalili, D., & Mahmoudi, Y. (2025). Physics-informed neural networks for two-phase film boiling heat transfer. *Int. J. Heat Mass Transf.*, 241, 126680. https://doi.org/10.1016/j.ijheatmasstransfer.2025.126680

[24] Wijerathne, A.D.H.T., *et al.* (2025). Recent advances in food drying modeling: empirical to multiscale physics-informed neural networks. *Compr. Rev. Food Sci. Food Saf.*, 24(3): e70194. https://doi.org/10.1111/1541-4337.70194

[25] Ye, B., *et al.* (2025). iMLGAM: Integrated machine learning and genetic algorithm-driven multiomics analysis for prediction. *Imeta*, 4(2): e70011. https://doi.org/10.1002/imt2.70011

[26] Alexakis, K., *et al.* (2025). Genetic algorithm-based multi-objective optimisation for energy-efficient systems: a systematic review. *Energy Build.*, 328, 115216. https://doi.org/10.1016/j.enbuild.2024.115216

[27] Zhang, W., *et al.* (2025). Multi-physics coupling model parameter identification using data-driven methods and genetic algorithms. *Energy*, 314, 134120. https://doi.org/10.1016/j.energy.2024.134120

[28] Adabbo, G., *et al.* (2025). A multi-objective optimization framework through genetic algorithm for hyperthermia-mediated drug delivery. *Comput. Biol. Med.*, 189, 109895. https://doi.org/10.1016/j.compbiomed.2025.109895

[29] Karkadakattil, A. (2025). AI-driven prediction of surface roughness in laser-polished LPBF Ti-6Al-4V: a sustainable proof-of-concept. *Austral. J. Multi-Disciplinary Eng.*, 1–13. https://doi.org/10.1080/14488388.2025.2570030

[30] Donachie, M.J. (2002). *Superalloys: A Technical Guide*. ASM International. https://doi.org/10.31399/asm.tb.stg2.9781627082679

[31] Davim, J.P. (2008). *Machining: Fundamentals and Recent Advances*. Springer.

[32] Groover, M.P. (2013). *Fundamentals of Modern Manufacturing: Materials, Processes, and Systems*. John Wiley & Sons.

[33] Davim, J.P. (2012). *Statistical and Computational Techniques in Manufacturing*. Springer. https://doi.org/10.1007/978-3-642-25859-6

[34] Li, T., *et al.* (2025). Experimental study on laser cutting of stainless steel hexagonal tube of reactor assemblies. *Nucl. Eng. Des.*, 432, 113788. https://doi.org/10.1016/j.nucengdes.2024.113788

[35] Zabon, A.H., Abbas, T.F., & Bedan, A.S. (2025). Enhancing laser cutting quality of stainless steel 201 using multi-factor design. *Adv. Sci. Technol. Res. J.*, 19(7): 458–470. https://doi.org/10.12913/22998624/204716

[36] Aziz, U., *et al.* (2025). Optimization of additively manufactured 316/316L stainless steel process parameters and post-processing strategies. *Materials*, 18(12): 2870. https://doi.org/10.3390/ma18122870

[37] Vishnulal, R., Govindan, P., & Vipindas, M. (2020). Laser machining of polymer materials: process challenges and strategies. In *Springer ICETE Proc.*, pp. 653–661. https://doi.org/10.1007/978-3-030-24314-2_77

[38] Karkadakattil, A. Geometry aware laser polishing of LPBF AlSi10Mg defence components with physics inspired neural network based surface roughness prediction. *Discov Mechanical Engineering* **4**, 52 (2025). https://doi.org/10.1007/s44245-025-00144-0

[39] Mousavian, R.T., *et al.* (2020). Development of BMG-B2 nanocomposite structure during laser surface processing. *Appl. Surf. Sci.*, 505, 144535. https://doi.org/10.1016/j.apsusc.2019.144535

[40] Patel, G.C.M., *et al.* (2021). Optimization of EDM parameters using hybrid Taguchi-based PCA and CRITIC approaches. *Metals*, 11(3): 10007.